RSC Advances

PAPER

View Article Online
View Journal | View Issue

Cite this: *RSC Adv.*, 2018, **8**, 33459

A simple and highly selective 1,2,4,5-tetrazine-based colorimetric probe for HSO_3^- ion recognition in food†

Jing Lu, Pei Wu, Yanxue Geng and Jianchun Wang *

A series of 3,6-bis-substituted-1,2,4,5-tetrazine-based colorimetric probes has been developed in good yields that exhibits highly selective and sensitive colorimetric recognition of HSO_3^- in aqueous solution. The color of the solution containing colorimetric probes changed markedly from orange to colorless, upon the addition of HSO_3^-. Quantification of the absorption titration analysis shows that the detection limit of 3,6-bis(2-aminoethylamino)-1,2,4,5-tetrazine (**2a**) for HSO_3^- was 3.8 μM. It was noted that 3,6-bis-substituted-1,2,4,5-tetrazine-based colorimetric probes have a specific response toward HSO_3^- without interference from other 17 different anions and 16 common cations. A plausible mechanism was proposed by high-resolution mass spectroscopy analysis and NMR spectrometry analysis, involving the nucleophilic reaction of a bisulfite anion with the tetrazine ring and free radical rearrangement of $\cdot SO_3H$. Moreover, probes **2a–2c** possessed applicability for sensing bisulfite in actual food samples. Therefore, the present work established a novel strategy for investigating bisulfite in food or other products.

Received 3rd July 2018
Accepted 21st September 2018

DOI: 10.1039/c8ra05682j

rsc.li/rsc-advances

Introduction

Sulfur dioxide (SO_2) is a pungent gas and major atmospheric pollutant that can easily be converted into its bisulfite (HSO_3^-) and sulfite (SO_3^{2-}) derivatives under humid conditions.[1,2] Owing to their ability to inhibit mildew and restrict microorganism growth, SO_2 derivatives are commonly used as preservatives and antioxidants in food, beverages, and drugs such as epinephrine.[3,4] Furthermore, endogenous sulfur dioxide derivatives are involved in many physiological processes.[5,6] For example, bisulfite generated in mitochondria reduces blood pressure and aids blood vessel dilation.[7] However, recent research has shown that a high bisulfite concentration in the body is not only correlated with the occurrence of allergic reactions,[8] but can also induce respiratory responses, neurological disorders, cardiovascular disease, and lung cancer.[9–12] Therefore, developing a highly sensitive and selective method for bisulfite detection is important for food safety, quality control, and human welfare.[13]

Currently, detection methods for HSO_3^- include titrimetry,[14] flow injection analysis, electrochemistry,[15] and spectroscopy.[16] Spectroscopy, which has innate advantages such as high sensitivity, good selectivity, and the low detection limits, is the most attractive among these methods.[17] Sensing mechanisms for HSO_3^- using spectroscopy include nucleophilic reactions with aldehydes,[18] Michael-type additions,[19,20] selective levulinate deprotection,[21] hydrogen bond formation,[22] and coordinative interactions.[23]

1,2,4,5-Tetrazines (or *s*-tetrazines) used in this paper are aromatic six-membered heterocycles containing four nitrogen atoms and bearing two electron-withdrawing amino substituents. The most prominent characteristic of *s*-tetrazines is their electron-deficient aromatic rings, which result from replacing four CH groups with four, more electronegative, nitrogen atoms on the prototypical aromatic ring.[24] Computational results have shown that *s*-tetrazines can be used as binding units for anion recognition.[25] Furthermore, the amino substituents cooperate with the four nitrogen atoms in the tetrazine ring to decrease the electron density of the carbon atoms at the 3 and 6 positions, making them susceptible to attack by nucleophilic reagents, such as HSO_3^-. Tetrazines are also colored due to a low-energy n–π* transition in the visible range, allowing them to be detected by the naked eye.[26]

Therefore, owing to the excellent optical and reaction properties of *s*-tetrazine, we developed novel 3,6-bis-substituted-1,2,4,5-tetrazine-based probes (**2a–2c**) for bisulfite anions. These probes can respond to HSO_3^- specifically and sensitively in aqueous solution and generate naked-eye detectable chromogenic and UV-Vis absorbance signaling. A corresponding mechanism is also proposed, as supported by the spectroscopic methods. Notably, the mechanism is unique and different from previously reported whole mechanisms. To our knowledge, this

Department of Chemistry, Capital Normal University, Beijing 100048, PR China. E-mail: cnuwjc@cnu.edu.cn; Fax: +86 10 68903040; Tel: +86 10 68902974-1

† Electronic supplementary information (ESI) available. See DOI: 10.1039/c8ra05682j

is the first study to use *s*-tetrazines as a probe for HSO_3^- anion recognition.

Experimental

Materials and methods

All materials and reagents were purchased from commercial suppliers and used without further purification. ^{1}H and ^{13}C NMR spectra were recorded on 600 MHz Varian VNMRS Spectrometer, using D_2O or DMSO-d_6 as solvent. High-resolution mass spectroscopy (HRMS) was performed on a Bruker APEXIIFT-ICR mass spectrometer. Melting points were measured on a WRS-1B micro-melting point apparatus (YiCe, Shanghai). Ultraviolet-visible (UV-Vis) spectra were recorded on Metash UV-8000s spectrophotometer. The pH values were measured using a PHS-3C digital pH meter (ShengCi, Shanghai).

Preparation for UV-Vis spectral measurements

As the probes showed excellent water solubility, experiments of **2a–2c** with HSO_3^- were conducted in aqueous solution. 4-(2-Hydroxyethyl)-1-piperazineethanesulfonic acid (HEPES) buffer (20 mM, pH 7.0) was used for UV-Vis measurements. Compounds **2a–2c** were separately dissolved in ultrapure water to obtain stock solutions (1 mM). Ultrapure water was also used to prepare stock solutions (10^{-2} M) of NaF, NaCl, KBr, NaI, NaOH, Na_2CO_3, $NaHCO_3$, Na_2SO_4, $KHSO_4$, Na_2SO_3, $NaHSO_3$, $NaNO_3$, $NaNO_2$, $Na_3PO_4\cdot12H_2O$, Na_2HPO_4, NaH_2PO_4, CH_3COONa, and $Na_2B_4O_7\cdot10H_2O$. Stock solutions of $NaHSO_3$ and Na_2SO_3 were freshly prepared before each use. In UV-Vis selectivity experiments, test solution was prepared by adding the stock solution of **2a**, **2b**, or **2c** (2 mL) into a 10 mL colorimetric tube, followed by 2 mL of one of the above analyte solutions, after which the test solution was made up to 10 mL using ultrapure water. For UV-Vis titration experiments, test solution was prepared by adding the stock solution of **2a**, **2b**, or **2c** (2 mL) into a 10 mL colorimetric tube with HEPES buffer (20 mM, pH 7.0), followed by a suitable volume of analyte solution, after which the test solution was made up to 10 mL using ultrapure water.

Determination of the detection limit

The detection limits were calculated from the UV-Vis titration results. UV-Vis spectra of **2a** were measured 20 times and the standard deviation of the blank measurement was determined. To obtain the slope, UV-Vis absorbance variations at 458 nm *vs.* HSO_3^- concentration were plotted, giving a linear graph. The detection limits were calculated using the equation $D = 3\sigma/k$, where σ is the standard deviation of the blank measurement, and k is the slope.

Synthesis of probes 2a–2c

Synthesis of 3,6-bis(2-aminoethylamino)-1,2,4,5-tetrazine (2a). The synthesis of **2a** was achieved following a previously reported procedure.[27]

Tetrazine **1** (0.300 g, 1.1 mmol) was added to ethylenediamine (3.5 mL). The resultant mixture was stirred at room temperature for 4 h. Excess diamine was removed under reduced pressure to afford a red precipitate. Toluene (5 mL) was added and the resultant precipitate was collected by filtration and washed with light petroleum. The crude product was purified by recrystallization from ethyl acetate to afford **2a** as a red powder (0.201 g, 92%), mp 133–135 °C. ^{1}H-NMR (600 MHz, D_2O, ppm) 3.48 (4H, t, $J = 6.1$ Hz), 2.87 (4H, t, $J = 6.1$ Hz). ^{13}C-NMR (151 MHz, D_2O, ppm) 159.84, 43.07, 39.46. HRMS (ESI) m/z calculated for $C_6H_{15}N_8^+$, 199.1414; found 199.1414.

Synthesis of 3,6-bis(3-aminopropylamino)-1,2,4,5-tetrazine (2b). Tetrazine **1** (0.300 g, 1.1 mmol) was added to 1,3-propanediamine (3.5 mL). The resultant mixture was stirred at room temperature for 4 h. Excess diamine was removed under reduced pressure to afford a red precipitate. Ether (15 mL) was added, the mixture was ultrasonicated, and the resultant red precipitate was collected by filtration and washed with ether multiple times. After further washing with light petroleum and filtration, **2b** was obtained as a pure red powder (0.178 g, 71.55%). Mp 103.8–106.6 °C. ^{1}H-NMR (600 MHz, D_2O, ppm) 3.41 (4H, t, $J = 6.9$ Hz), 2.72 (4H, t, $J = 7.1$ Hz), 1.78 (4H, q, $J = 7.0$ Hz). ^{13}C-NMR (151 MHz, D_2O, ppm) 159.66, 38.66, 38.02, 30.85. HRMS (ESI) m/z calculated for $C_8H_{19}N_8^+$, 227.1727; found 227.1719.

Synthesis of 3,6-bis(3-aminobutylamino)-1,2,4,5-tetrazine (2c). Tetrazine **1** (0.300 g, 1.1 mmol) was added to 1,4-butanediamine (3.5 mL). The resultant mixture was stirred at 35 °C for 6 h. Excess diamine was removed under reduced pressure to afford a red precipitate. Ether (15 mL) was added, the mixture was ultrasonicated, and the resultant red precipitate was collected by filtration and washed with ether multiple times. After further purification by heating circumfluence with light petroleum and filtration, **2c** was obtained as a pure red powder (0.204 g, 72.85%). Mp 113.2–115.8 °C. ^{1}H-NMR (600 MHz, D_2O, ppm) 3.40 (4H, t, $J = 6.9$ Hz), 2.73 (4H, t, $J = 7.2$ Hz), 1.70–1.64 (4H, m), 1.61–1.54 (2H, m).^{13}C-NMR (151 MHz, DMSO-d_6, ppm) 160.84, 41.90, 41.21, 31.23, 26.65. HRMS (ESI) m/z calculated for $C_{10}H_{23}N_8^+$, 255.2040; found 255.2032.

Synthesis of compound 3a–3c

A mixture of **2a** (0.200 g, 1 mmol) and $NaHSO_3$ (0.2289 g, 2.2 mmol) in distilled water (10 mL) was stirred at room temperature for 20 min. The solvent was then removed under reduced pressure, methanol (10 mL) was added, and the mixture was filtered. The filtrate was evaporated under reduced pressure to afford **3a** as a white powder. (0.2564 g, 71.00%). ^{1}H-NMR (600 MHz, D_2O, ppm) 3.56 (4H, t, $J = 5.8$ Hz), 3.22 (4H, t, $J = 5.7$ Hz). ^{13}C-NMR (151 MHz, D_2O, ppm) 152.16, 40.01, 38.57. HRMS (ESI) m/z calculated for $C_6H_{17}N_8O_6S_2^+$, 361.0707; found 361.0706.

3b and **3c** were synthesized in a similar way to **3a**.

3b. ^{1}H-NMR (600 MHz, D_2O, ppm) 3.22 (2H, t, $J = 6.6$ Hz), 3.11 (2H, t, $J = 6.5$ Hz), 2.95–2.91 (4H, m), 1.87–1.77 (4H, m). ^{13}C-NMR (151 MHz, D_2O, ppm) 154.08, 148.77, 38.57, 38.45,

37.12, 36.68, 26.57, 25.89. HRMS (ESI) *m*/*z* calculated for $C_8H_{19}N_8O_6S_2^-$, 387.0880; found 387.0874. (Fig. S1–S3†).

3c. ^{1}H-NMR (600 MHz, D_2O, ppm) 3.29 (2H, t, J = 6.5), 3.18 (2H, t, J = 6.6), 3.03 (4H, m, J = 14.6, 6.5 Hz), 1.74 (4H, m, J = 15.3, 7.6 Hz), 1.71–1.64 (4H, m). ^{13}C-NMR (151 MHz, D_2O, ppm) 149.19, 41.01, 40.85, 39.09, 38.97, 25.40, 24.65, 24.20, 23.86. HRMS (ESI) *m*/*z* calculated for $C_{10}H_{25}N_8O_6S_2^+$, 417.1325; found 417.1333. (Fig. S4–S6†).

Results and discussion

Probes **2a–2c** were easily prepared in good yields (Scheme 1) and the structures were characterized by ^{1}H and ^{13}C NMR, and high-resolution mass spectrometry (HRMS) (Fig. S7–S15†).

UV-Vis absorption spectra of detecting HSO_3^-

UV-Vis titration spectra experiments for HSO_3^- in aqueous solution (HEPES buffer: 20 mM, pH7.0) were conducted using solutions containing different HSO_3^- concentrations. As shown in Fig. 1a, with increasing sulfite concentration, the absorbance at 458 nm decreased gradually. As expected, when the HSO_3^- concentration reached 2.0 equiv., the ΔAbs(A_0 − A) reached a maximum and then plateaued (Fig. 1b). These experimental results coincided with the mechanistic analysis that a 1 : 2 adduct was generated. Furthermore, the orange solution changed to colorless, allowing the colorimetric detection of HSO_3^- by the naked eye.

The selective response of probe 2a to HSO_3^-

The selectivity of **2a** for HSO_3^- over other anions was investigated in aqueous solution at ambient temperature. As shown in Fig. 2a, free probe **2a** showed a UV-Vis absorption centered at 458 nm. When 10 equiv. of 18 different representative anions (F^-, Cl^-, Br^-, I^-, OH^-, CO_3^{2-}, HCO_3^-, SO_4^{2-}, HSO_4^-, SO_3^{2-}, HSO_3^-, NO_3^-, NO_2^-, PO_4^{3-}, HPO_4^{2-}, $H_2PO_4^-$, CH_3COO^-, and $B_4O_7^{2-}$) were added to the aqueous solution, only HSO_3^- induced a significant color change from orange to colorless (Fig. 2c), while others triggered only minor changes. Upon HSO_3^- addition, the absorption centered at 458 nm as diminished, meaning that colorimetric detection of HSO_3^- could be observed by the naked eye. Probes **2b** and **2c** showed similar sensing phenomena for HSO_3^- (Fig. S16 and S17†). But with the increasing length of chains, the selective efficiency is reduced obviously, response time is much longer and the reverse reactions between **2b** and **3b**, **2c** and **3c** happened easier, which leads to decreasing of the linearity of absorbance efficiency and concentration (Fig. S18 and S19†). And also the solubility in water decreases. Furthermore, competition experiments

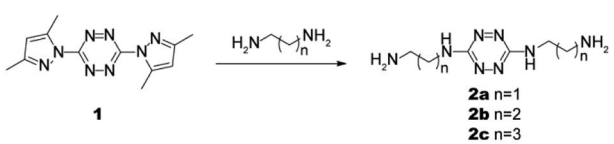

Scheme 1 Design and synthesis of probes **2a–c**.

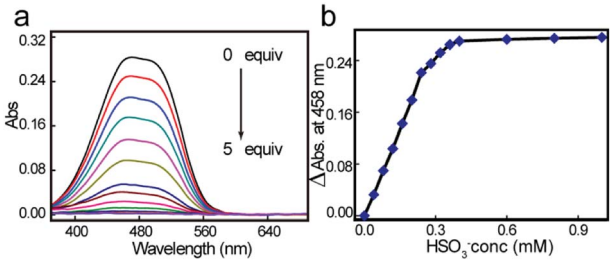

Fig. 1 UV-Vis titration spectra (a) and ΔAbs (A_0 − A) *vs.* bisulfite concentration plot (b) of **2a** (2.0×10^{-4} M) toward 0 to 5 equiv of HSO_3^- in HEPES buffer (pH 7.0, 20 mM, 100% ultrapure water).

confirmed the good HSO_3^- selectivity. As shown in Fig. 2b, in the presence of the competitive species mentioned above, the signaling of **2a** toward HSO_3^- was not affected. Additionally, **2a** showed a negligible response to 16 different representative cations (Fig. S20†), suggesting that cations will not interfere with the probe **2a**. These results implied that the novel probes (**2a–2c**) had excellent selectivity for HSO_3^- over other anions in aqueous environment.

pH dependent

We also explored the effect of pH on HSO_3^- determination. The maximum absorbance obtained at 458 nm for free probe **2a** and probe **2a**–HSO_3^- at different pH values is shown in Fig. 3. The absorbance of free **2a** was constant at pH 5.5–9.5, indicating that it was stable. After adding 4.0 equiv. of HSO_3^-, the absorbance decreased, with a maximum value in the pH range 5.5–7.5. As both alkaline and acidic solutions would block HSO_3^- formation, we chose a neutral pH for further studies.

The detection limit of probe 2a for HSO_3^-

According to concentration-dependent signaling behavior, the absorbance at 458 nm decreased linearly (0.9947) when the concentration of HSO_3^- ranged from 0 to 20 μM (Fig. 4a and b). The detection limit for HSO_3^- was estimated as 3.8 μM.

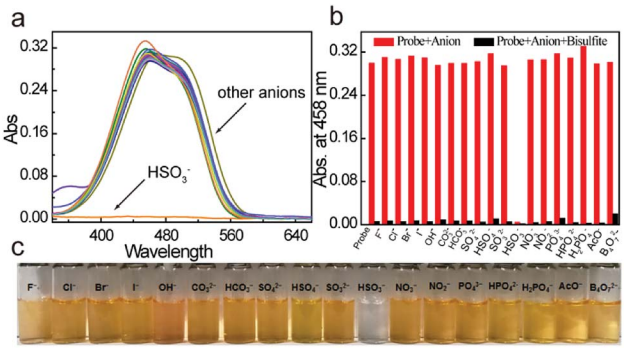

Fig. 2 (a) UV-Vis spectra of probe **2a** in the presence of common anions. [**2a**] = 2.0×10^{-4} M, [An^-] = 2.0×10^{-3} M. λ_{max} = 458 nm. (b) Competition experiments of the **2a**–sulfite system and (c) color change photograph in the presence of coexisting anions. [**2a**] = 2.0×10^{-4} M. [Bisulfite] = 2.0×10^{-3} M. [An^-] = 2.0×10^{-3} M. All spectra were measured in 100% ultrapure water.

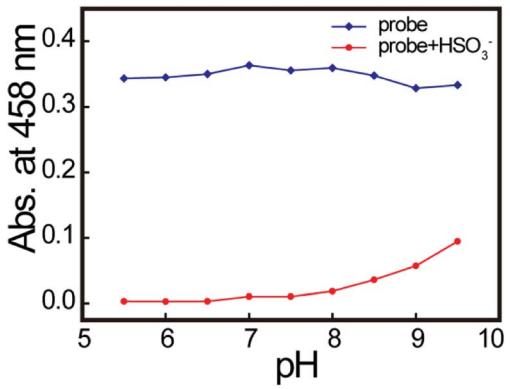

Fig. 3 Effect of test solution pH on **2a** (2.0×10^{-4} M) in the absence (blue line) or presence (red line) of bisulfite (4 equiv.).

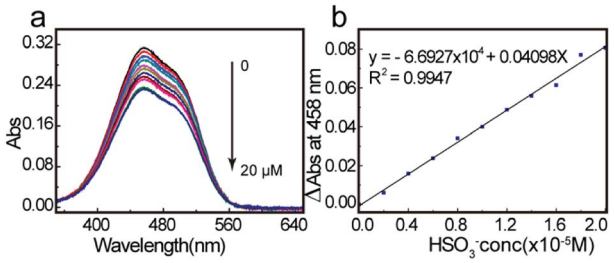

Fig. 4 UV-Vis spectra (a) and ΔAbs ($A_0 - A$) *vs.* bisulfite concentration plot for detection limit determination (b) of probe **2a** in the presence of HSO_3^- at concentrations ranging from 0 to 20 μM. [**2a**] = 2.0×10^{-4} M. In HEPES buffer (pH 7.0, 20 mM, 100% ultrapure water).

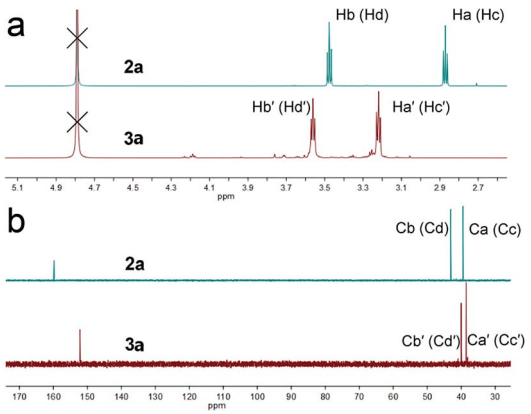

Fig. 5 (a) ^{1}H and (b) ^{13}C NMR spectra of **2a** in D_2O and **2a**–$NaHSO_3$ in D_2O.

Proposed mechanism

The change in chromogenic signaling showed that the π-conjugated structure of *s*-tetrazine was disrupted, with a new compound (**3a**) formed, which was obtained by performing the reaction on a large scale.

Clean ^{1}H and ^{13}C NMR, and HRMS, spectra of **3a** were obtained (Fig. S21–S23†). As shown in Fig. 5a, the proton signals at 2.87 and 3.48 ppm were assigned to the methylene protons H_a (H_c) and H_b (H_d), respectively, in **2a**. Upon addition of HSO_3^- to a D_2O solution of **2a**, all proton peaks shifted downfield. Resonance signals of H_a and H_c at around 2.87 ppm shifted to 3.22 ppm (H_a', H_c'; $\delta = 0.35$ ppm) and resonance signals of H_b and H_d at about 3.48 ppm shifted to 3.56 ppm (H_b', H_d'; $\delta = 0.08$ ppm). Furthermore, as shown in Fig. 5b, the chemical shifts of carbon atoms at the 3 and 6-positions shifted from 159.84 to 152.16 ($\delta = 7.67$ ppm), while that of C_a (C_c) shifted from 39.46 to 38.57 ($\delta = 0.89$ ppm) and C_b (C_d) shifted from 43.07 to 40.01 ($\delta = 3.06$ ppm). All changes in the ^{1}H NMR spectra were attributed to the formation of O···H hydrogen bonds between the sulfonic acid and methylene groups bonded to the carbon atoms in the tetrazine ring. In contrast, the collapse of the tetrazine conjugate system in compound **3a** reduced the inductive effect of nitrogen atoms on tetrazine, leading to ^{13}C NMR signals shifting upfield. The parent ion peak at *m*/*z* 361.0706 ($[M + H]^+$) also strongly supported the formation of **3a**.

When free radical inhibitor, 2,2,6,6-tetramethylpiperidine-1-oxyl (Tempo) was added in the reaction, the color changed from orange to colorless as normal. It manifests that the mechanism is not free radical type at first. Based on the experimental fact and spectral data, a mechanism was proposed (Scheme 2). Two tautomeric forms of HSO_3^- exist in dynamic equilibrium, one with a proton attached to sulfur (HSO_3^-) and the other protonated at oxygen ($HOSO_2^-$). The latter has two equivalent resonance structures. The carbon atoms in the tetrazine ring connected to three nitrogen atoms were electron deficient and easily attacked by nucleophile HSO_3^-. Formation of a sulfur–carbon bond leads to the collapse of the tetrazine conjugate system and formation of intermediate **I**. But the steric hindrance at 3,6-positions makes the **I** unstable to split into $\cdot SO_3H$ and free radicals **II**, followed by formation of more stable free radicals **III**. At last compound **3a** was obtained by formation of C–S bond.

Detection of HSO_3^- in realistic food samples

Encouraged by these results, we also explored whether probe **2a** shows a response for HSO_3^- in realistic food samples. We detected HSO_3^- in dry white wine, corn starch, canned fruit and

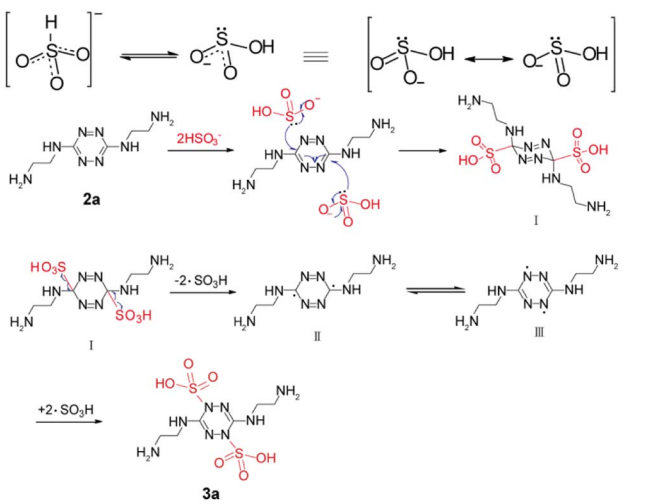

Scheme 2 Proposed formation mechanism of **3a**.

Table 1 Determination of HSO_3^- in various food samples

Sample	HSO_3^- level (μM)	Added (μM)	Found (μM)	Recovery (%)
Dry white wine	14.27	3.00	16.02	92.8%
Corn starch	11.07	3.00	15.10	107.3%
Canned fruit	15.85	3.00	19.05	101.1%
Jasmine tea drinks	15.76	3.00	18.93	100.9%

jasmine tea drinks, which were purchased from a local supermarket. As shown in Table 1, **2a** was able to determine HSO_3^- concentration in these samples with good recovery, ranging from 92.8% to 107.3%. The levels of HSO_3^- were calculated to be 38.56, 2.49, 3.21 and 2.13 mg kg^{-1}, respectively. Moreover, titration method was also used to determine the concentration of HSO_3^- (Table S1†). However, the determination values in corn starch, canned fruit and jasmine tea drinks by iodine titration method were much higher than the values in this method, due to the reducing substances and only the results of dry white wine agreed well with our method. Thus, our method has advantages over traditional titration method for complex samples. Probe **2a** could be well applied in the detection of HSO_3^- in food products.

Conclusions

In summary, we have developed novel 3,6-bis-substituted-1,2,4,5-tetrazine-based probes (**2a–2c**). The probes exhibited a colorimetric response to HSO_3^- with excellent selectivity and good sensitivity in neutral aqueous solution at ambient temperature. Thus, probes **2a–2c** possessed applicability for sensing bisulfite in actual food samples. A plausible mechanism was proposed, involving the nucleophilic reaction of a bisulfite anion with the tetrazine ring, followed by rearrangement of $\cdot SO_3H$.

Conflicts of interest

There are no conflicts to declare.

Acknowledgements

This work was supported by the General Plan of Beijing Municipal Education Commission [grant number KM201710028007]; and the Beijing Natural Science Foundation [grant numbers 2173060].

References

1 A. V. Leontiev and D. M. Rudkevich, *J. Am. Chem. Soc.*, 2005, **127**, 14126–14127.
2 S. Wang, X. Cao, T. Gao, X. Wang, H. Zou and W. Zeng, *Mikrochim. Acta*, 2018, **185**, 218.
3 L. Zhu, J. Xu, Z. Sun, B. Fu, C. Qin, L. Zeng and X. Hu, *Chem. Commun.*, 2015, **51**, 1154–1156.
4 J. Wang, Y. Hao, H. Wang, S. Yang, H. Tian, B. Sun and Y. Liu, *J. Agric. Food Chem.*, 2017, **65**, 2883–2887.
5 T. Yu, G. Yin, T. Niu, P. Yin, H. Li, Y. Zhang, H. Chen, Y. Zeng and S. Yao, *Talanta*, 2018, **176**, 1–7.
6 D. P. Li, Z. Y. Wang, X. J. Cao, J. Cui, X. Wang, H. Z. Cui, J. Y. Miao and B. X. Zhao, *Chem. Commun.*, 2016, **52**, 2760–2763.
7 J. Xu, J. Pan, X. Jiang, C. Qin, L. Zeng, H. Zhang and J. F. Zhang, *Biosens. Bioelectron.*, 2016, **77**, 725–732.
8 X. Ma, C. X. Liu, Q. L. Shan, G. H. Wei, D. B. Wei and Y. G. Du, *Sens. Actuators, B*, 2013, **188**, 1196–1200.
9 W. Zhang, T. Liu, F. Huo, P. Ning, X. Meng and C. Yin, *Anal. Chem.*, 2017, **89**, 8079–8083.
10 S. Samanta, P. Dey, A. Ramesh and G. Das, *Chem. Commun.*, 2016, **52**, 10381–10384.
11 Y. Liu, K. Li, M. Y. Wu, Y. H. Liu, Y. M. Xie and X. Q. Yu, *Chem. Commun.*, 2015, **51**, 10236–10239.
12 Y. Q. Sun, J. Liu, J. Zhang, T. Yang and W. Guo, *Chem. Commun.*, 2013, **49**, 2637–2639.
13 M. G. Choi, J. Hwang, S. Eor and S. K. Chang, *Org. Lett.*, 2010, **12**, 5624–5627.
14 D. Lowinsohn and M. Bertotti, *Food Addit. Contam.*, 2001, **18**, 773–777.
15 S. S. Hassan, M. S. Hamza and A. H. Mohamed, *Anal. Chim. Acta*, 2006, **570**, 232–239.
16 H. Li, X. Zhou, J. Fan, S. Long, J. Du, J. Wang and X. Peng, *Sens. Actuators, B*, 2018, **254**, 709–718.
17 D. P. Li, Z. Y. Wang, H. Su, J. Y. Miao and B. X. Zhao, *Chem. Commun.*, 2017, **53**, 577–580.
18 X. H. Cheng, H. Z. Jia, J. Feng, J. G. Qin and Z. Li, *Sens. Actuators, B*, 2013, **184**, 274–280.
19 J. Luo, G. J. Song, X. J. Xing, S. L. Shen, Y. Q. Ge and X. Q. Cao, *New J. Chem.*, 2017, **41**, 3986–3990.
20 S. Xu, R. Tang, Z. Wang, Y. Zhou and R. Yan, *Spectrochim. Acta, Part A*, 2015, **149**, 208–215.
21 Y. Sun, Y. Li, X. Ma and L. Duan, *RSC Adv.*, 2016, **6**, 79830–79835.
22 L. Wang, W. X. Li, W. J. Zhi, D. D. Ye, Y. Wang, L. Ni and X. Bao, *Dyes Pigm.*, 2017, **147**, 357–363.
23 Y. Q. Sun, P. Wang, J. Liu, J. Zhang and W. Guo, *Analyst*, 2012, **137**, 3430–3433.
24 Y. Sun, C. Zhong, R. Gong, H. Mu and E. Fu, *J. Org. Chem.*, 2009, **74**, 7943–7946.
25 Y. Zhao, Y. Li, Z. Qin, R. Jiang, H. Liu and Y. Li, *Dalton Trans.*, 2012, **41**, 13338–13342.
26 Y. H. Gong, M. Fabien, M. R. Rachel, B. Sophie, L. Galmiche, J. Tang, P. Audebert and G. Clavier, *Eur. J. Org. Chem.*, 2009, **2009**, 6121–6128.
27 C. Glidewell, P. Lightfoot, B. J. L. Royles and D. M. Smith, *J. Chem. Soc., Perkin Trans. 2*, 1997, **0**, 1167–1174.